ACCOUNTS
of chemical research

Molecular Rotors: What Lies Behind the High Sensitivity of the Thioflavin-T Fluorescent Marker

NADAV AMDURSKY,[†] YUVAL EREZ,[‡] AND DAN HUPPERT*,[‡]

[†]*Department of Materials and Interfaces, Faculty of Chemistry, Weizmann Institute of Science, Rehovot, 76100, Israel, and* [‡]*Raymond and Beverly Sackler Faculty of Exact Sciences, School of Chemistry, Tel Aviv University, Tel Aviv 69978, Israel*

RECEIVED ON FEBRUARY 16, 2012

CONSPECTUS

Thioflavin-T (ThT) can bind to amyloid fibrils and is frequently used as a fluorescent marker for *in vitro* biomedical assays of the potency of inhibitors for amyloid-related diseases, such as Alzheimer's disease, Parkinson's disease, and amyloidosis. Upon binding to amyloid fibrils, the steady-state (time-integrated) emission intensity of ThT increases by orders of magnitude. The simplicity of this type of measurement has made ThT a common fluorescent marker in biomedical research over the last 50 years.

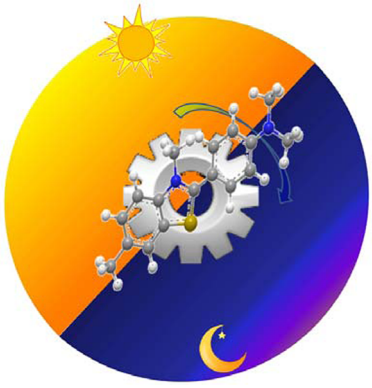

As a result of the remarkable development in ultrafast spectroscopy measurements, researchers have made substantial progress in understanding the photophysical nature of ThT. Both *ab initio* quantum-mechanical calculations and experimental evidence have shown that the electronically excited-state surface potential of ThT is composed of two regimes: a locally excited (LE) state and a charge-transfer (CT) state. The electronic wave function of the excited state changes from the initial LE state to the CT state as a result of the rotation around a single C−C bond in the middle of the molecule, which connects the benzothiazole moiety to the dimethylanilino ring. This twisted-internal-CT (TICT) is responsible for the molecular rotor behavior of ThT.

This Account discusses several factors that can influence the LE-TICT dynamics of the excited state. Solvent, temperature, and hydrostatic pressure play roles in this process. In the context of biomedical assays, the binding to amyloid fibrils inhibits the internal rotation of the molecular segments and as a result, the electron cannot cross into the nonradiative "dark" CT state. The LE state has high oscillator strength that enables radiative excited-state relaxation to the ground state. This process makes the ThT molecule light up in the presence of amyloid fibrils.

In the literature, researchers have suggested several models to explain nonradiative processes. We discuss the advantages and disadvantages of the various nonradiative models while focusing on the model that was initially proposed by Glasbeek and co-workers for auramine-O to be the best suited for ThT. We further discuss the computational fitting of the model for the nonradiative process of ThT.

1. Introduction

Thioflavin-T (ThT) (Scheme 1) was first introduced as a fluorescent marker for amyloid fibrils in 1965.[1] The steady-state fluorescence of ThT (usually measured at an emission wavelength of 482 nm) increases by more than 2 orders of magnitude upon binding to amyloid fibrils. The different characteristics in the bound to fibrils state and the different binding constant for different amyloid fibrils make ThT an important tool for fibril structure investigation.[2,3] Because of the simplicity of the measurement, ThT has become a standard for the *in vitro* quantification of amyloid formation, and it is usually used for measuring the potency and kinetics of inhibitors for amyloid-related neurodegenerative diseases, such as Alzheimer's, Parkinson's, type II diabetes, and more.[4−9] Figure 1 shows the steady-state and time-resolved emission of ThT before and after the formation of insulin amyloid fibrils and the dynamics of the insulin-fibrillization process. Over the years, it has been

Published on the Web 06/27/2012 www.pubs.acs.org/accounts
10.1021/ar300053p © 2012 American Chemical Society

SCHEME 1

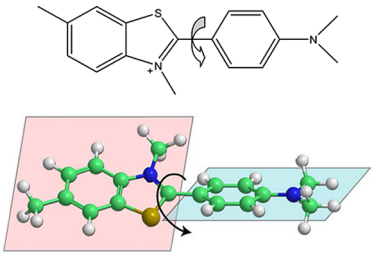

Reprinted with permission from ref 17. Copyright 2010 Elsevier B.V

found that ThT can also bind to DNA.[10,11] In addition, its on–off fluorescence regulation can be induced by cyclodextrin,[12] cucurbit[*n*]uril,[13] polymer membranes,[14] SDS micelles[15] and, as recently shown, porous silicon.[16]

For a long time, the main discussion in the literature regarding ThT has dealt with the molecular mechanism by which it interacts with different amyloid fibrils.[17−22] In this context, it was found, first by angle-dependent emission technique (the Krebs model[21]) and later confirmed by molecular modeling and near-field scanning optical microscopy measurements,[23] that ThT should bind to the amyloid fibril in parallel to the axis of the fibril in order to serve as a fluorescent marker.[21] Much less attention has been paid to the following questions: why is ThT such a remarkable fluorescent marker and what are the photophysical properties that enable it to achieve that ability? As a result of the vast progress in ultrafast spectroscopic techniques over the last decades, these questions may now be addressed. In this Account, we will review the photophysical properties of ThT, which underlie its ability as a fluorescent marker.[4−9]

2. Steady-State and Time-Resolved Emission of ThT

All of the aforementioned biomedical applications of ThT are derived from its on–off mechanism upon binding to another molecule, and its fluorescence-intensity dependence on the concentration of the examined molecules (usually amyloid fibrils). Although some studies were made earlier on the photophysical properties of unbound ThT,[24] the first one to point out the importance of the solvent viscosity to the fluorescence properties was Voropai et al.,[25] but only since 2007 has real progress in this field been made. Maskevich et al.[26] and Naik et al.[27] showed that the absorption maximum, the steady-state fluorescence, the excitation- and emission-peak locations, and the quantum yield of ThT all vary significantly as a function of the solvent properties (Table 1). The photophysical-measurement

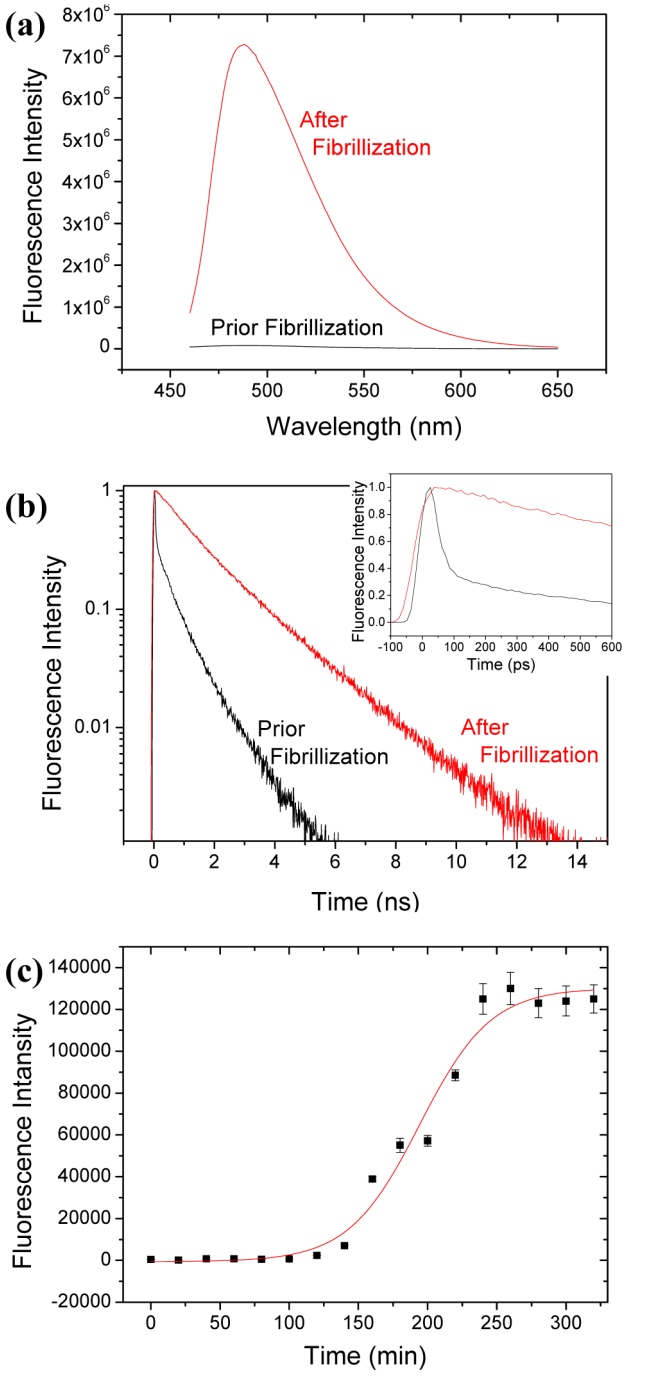

FIGURE 1. Spectroscopic properties of ThT upon binding to insulin amyloid fibrils: (a) steady state, (b) time-resolved, and (c) dynamics of the fibrillization process. Results acquired by N. Amdursky.

parameters of ThT can also be altered by varying the viscosity of the solution, as was done with glycerol–water[28,29] and acetonitrile–ethylene glycol[30] solvent mixtures (Figure 2a). The viscosity and the dielectric constant of the solution can also be controlled by changing the hydrostatic pressure and the temperature of the solution, respectively. Stsiapura et al. found a decrease in the quantum yield

TABLE 1. Spectral Properties of ThT in Several Solvents

			emission maxima (nm)				
			excitation wavelength (nm)				
solvent	solvent polarity function	abs maxima (nm)	418	440	Stokes shift (cm^{-1})[a]	quantum yield	ref
water	0.32	412	489	493	3990	3×10^{-4}	26,27
methanol	0.31	416	487	488	3550	4×10^{-4}	26,27
2-propanol	0.28	418	501	488	3430	2.5×10^{-3}	26,27
ethanol	0.29	418		490	3510	1.2×10^{-3}	26,27
acetone	0.28	415		489	3650	3×10^{-4}	26
acetonitrile	0.31	416	487	493	3760	2×10^{-4}	26
chloroform	0.15	424	481	490	3170	0.0113	26,27
1-butanol	0.26	418	478	489	3470	4.3×10^{-3}	26,27
dmso	0.26	418	501	503	4040	9×10^{-4}	26,27
dichloromethane	0.22	430	484		2594	0.0107[b]	26,27
glycerol	0.26	421	490	493	3470	0.0992	27
1-octanol	0.23	419		488	3380	0.0139	26,28
ethylene glycol	0.28	420		496	3650		26
dimethylformamide	0.28	417		496	3820	6×10^{-4}	26
pyridine	0.21	426		496	3310		26

[a]The Stoke's shift was calculated for an excitation wavelength of 440 nm, except for dichloromethane, which was calculated for a wavelength of 418 nm. [b]The reported relative quantum yield was corrected by comparison to chloroform.

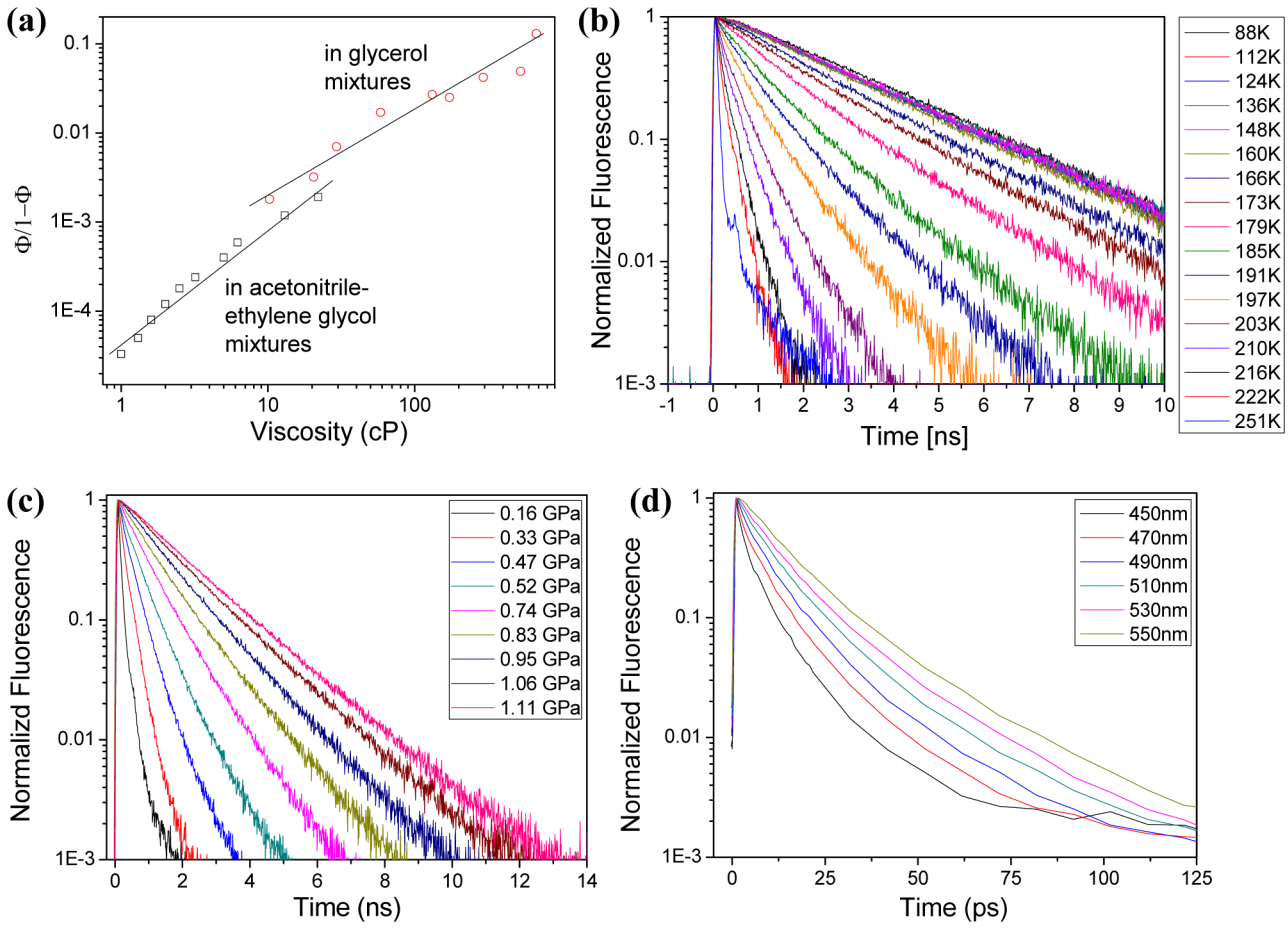

FIGURE 2. (a) Quantum yield of ThT as a function of viscosity in mixtures of glycerol (red circles) and acetonitrile−ethylene glycol (black squares). Changes in the time-resolved emission as a function of (b) temperature (in propanol) and (c) pressure (in pentanol) (for b and c, $\lambda_{ex} = 390$ nm, $\lambda_{em} = 490$ nm). (d) Time-resolved emission of ThT in propanol measured at several wavelengths by fluorescence up-conversion technique ($\lambda_{ex} = 390$ nm). Reprinted with permission from refs 31 and 32. Copyright 2011 American Chemical Society.

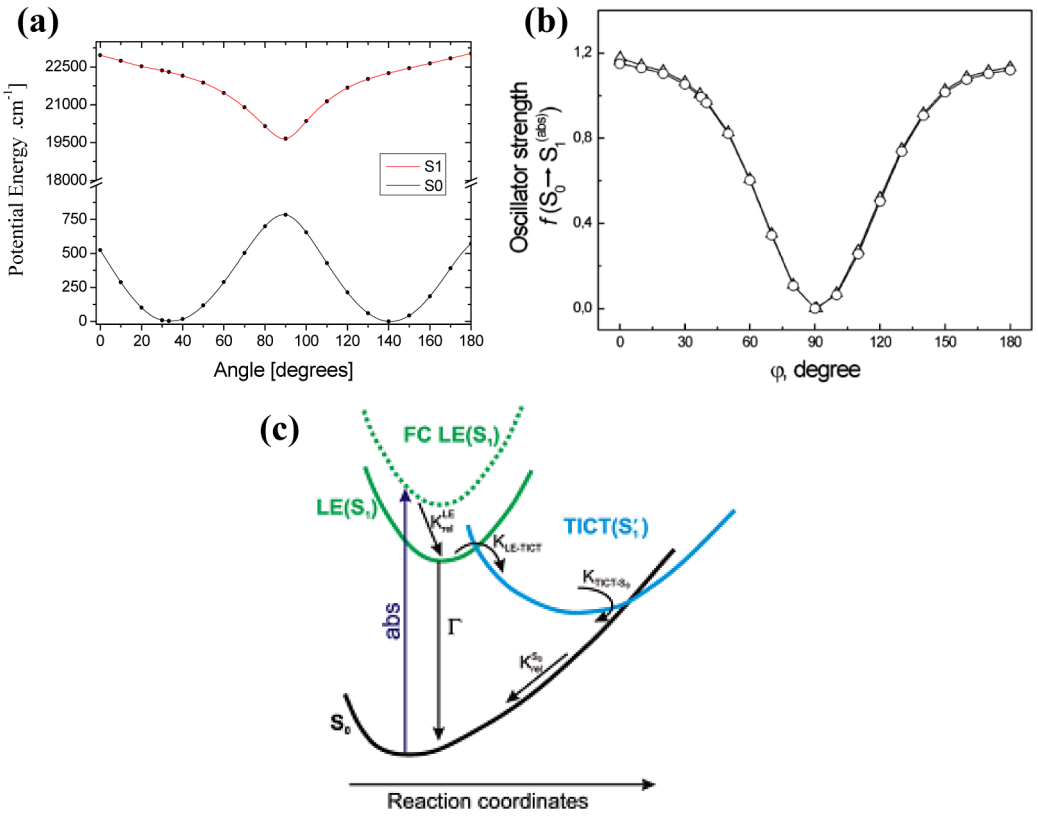

FIGURE 3. (a) Potential-energy curves of ThT ground and first excited states and (b) the oscillator strength as a function of the dihedral angle. (c) Excited-state-relaxation schemes of ThT. Reprinted with permission from refs 36−38. Copyright 2007, 2010, and 2011 American Chemical Society.

of ThT following the heating of a solution of ThT in 99% glycerol over a relatively small range of temperatures (270−330 K).[28] Recently, Huppert et al. found a large variation in the time-resolved emission of ThT in propanol over a temperature range of 80−270 K[31] (Figure 2b) and hydrostatic pressure on viscous solvents in the range of 0.15−2 GPa[32] (Figure 2c). Nath et al.[33] showed that in confined water/aerosol-OT/oil reverse micelles, the quantum yield of ThT increases by ∼250-fold over that of ThT in bulk water. The decrease in quantum yield with increase in pool size of the reverse micelles was shown to be nonlinear. In the context of binding to amyloid fibrils, it was shown recently that the fluorescence quantum yield of ThT bound to amyloid fibrils can be smaller or larger than that of ThT in rigid isotropic solution.[2,3,34]

Ultrafast up-conversion techniques have allowed researchers to follow the time-resolved emission of ThT in protic alcohol solvents[30−32] and even in water[35] at room temperature, where ThT has a low quantum yield of 0.0003.[26] Under these conditions, the emission lifetime of ThT (at the detection wavelength of 490 nm) ranges from ∼1 ps in water to ∼25 ps in 1-pentanol.

It is important to notice that no matter the solvent, temperature, or pressure of the solution, the time-resolved emission of ThT strongly depends on the detected emission wavelength and always exhibits a nonexponential profile (a concave shape of the decay curves at all wavelengths),[30−32,35] as can be seen in the example of the up-conversion measurements of ThT in propanol (Figure 2d). The time-resolved emission of many dyes exhibits wavelength dependence, which is usually interpreted as solvation dynamics, occurring around a molecule in the excited state that was prepared by a short pulse. Nath et al.[30,35] used this interpretation for the wavelength dependence of the ThT time-resolved emission. However, the interpretation is probably more complex and involves also the nonradiative process, initiated by intramolecular rotation of the ring subunits, that leads to the short emission lifetime of ThT in general and at long wavelength in particular. Later in this Account, we will discuss the complete nonradiative model that accounts for the wavelength dependence, the concave shape, and the short lifetime of the long wavelength time-resolved emission signals.

3. Nonradiative Processes of ThT

So, why is ThT such a remarkable fluorescent marker? It appears that the explanation derives from the electronic structure of the molecule. *Ab initio* quantum-chemical

TABLE 2. The Nonradiative Kinetic Parameter of ThT in Several Solvents

solvent	viscosity (cP)	$k_{LE\text{-}TICT}$ (s^{-1})	$k_{TICT\text{-}S_0}$ (s^{-1})	ref
water	0.9	7.69×10^{11} [a]	2.63×10^{11} [a]	26
ethanol	1.1	2.17×10^{11} [a]	3.57×10^{10} [a]	38
1-propanol	1.9	1.43×10^{11} [b]		38
2-propanol	2.1	1.56×10^{11} [a]	1.43×10^{10} [a]	32
1-butanol	2.7	7.69×10^{10} [c]	2.78×10^{9} [a]	38
		8.47×10^{10} [a]		32
1-pentanol	3.5	4.76×10^{10} [c]		38

[a] $\lambda_{ex} = 390$ nm; $\lambda_{em} = 490$ nm. [b] $\lambda_{ex} = 395$ nm; $\lambda_{em} = 510$ nm. [c] $\lambda_{ex} = 395$ nm; $\lambda_{em} = 490$ nm.

calculations performed first by Voropai et al.[25] and later by Stsiapura et al.[36] led to the conclusion that rotation around a single C−C bond in ThT (the one connecting the benzothiazole moiety to the dimethylanilino ring, marked by an arrow in Scheme 1) is responsible for the nonradiative decay rate of the molecule. These calculations also predict that the charge transfer due to the internal rotation between the two molecular fragments is favorable in energy. Since then, several other investigators have also reported on the quantum-chemical calculations of the ground and excited electronic states of ThT as a function of the dihedral angle of this bond (Figure 3a).[28,30,35,37] It was found in these calculations that the electronic ground state of ThT, S_0, falls sharply by $\sim$1500 cm^{-1} from a maximum located at the dihedral angle of $\varphi = 90°$ to a minimum at $\varphi = 37°$. The 37° angle for which the potential-energy minimum is obtained, is a compromise between the coplanar conformer, favored by the "electronic effects" and the steric disturbance by the methyl group. On the other hand, the minimum of the ThT excited singlet state, S_1, is at $\varphi = 90°$. Hence, when undisturbed, the excited electronic state begins from the radiative locally excited (LE) state at the dihedral angle of $\varphi = 37°$ and crosses to a nonradiative twisted internal charge-transfer (TICT) state at the dihedral angle of $\varphi = 90°$. As a result, the oscillator strength also drops significantly from an initial value of $\sim$1.1 at $\varphi = 37°$ to a low value of $\sim$0.01 at $\varphi = 90°$ (Figure 3b). The fluorescence intensity controlled by the dihedral angle of the C−C bond is what defines ThT as a molecular rotor.

3.1. Ground and Excited Electronic-Potential Curves. In a later work of Stsiapura et al.,[38] a femtosecond transient-absorption technique was used to follow the electronic-state dynamics of ThT dissolved in low-viscosity solvents (water, ethanol, 2-propanol, and butanol) at room temperature. The observed lifetime of the LE state was in the range of a few picoseconds, from $\sim$1.3 ps (for water) to $\sim$12 ps (for butanol). However, the repopulation of the ground state from the excited TICT state has much larger time-constant values, from $\sim$4 ps (for water) to $\sim$360 ps (for butanol). According to the lifetimes obtained, they proposed the scheme for the excited-state deactivation of ThT (Figure 3c). In this scheme, the solvent relaxation processes from the nonequilibrium Franck−Condon state are denoted by k_{ref}^{LE}. Γ refers to the radiative transition to the ground state. $k_{LE\text{-}TICT}$ refers to the charge-transfer rate constant from the radiative LE state to the nonemissive (dark) TICT state. The transition rate constant from the LE to the TICT state exceeds 10^{11} s^{-1} in the low-viscosity solvents examined. $k_{TICT\text{-}S_0}$ refers to the rate constant of TICT deactivation to the ground state (S_0) via a conical intersection between the TICT (S_1') state to the ground state. The high sensitivity of both processes to the viscosity of the solution will be discussed in detail in the next section. Values of the rate constant, $k_{TICT\text{-}S_0}$, of 2.6×10^{11} s^{-1} (for water) to 2.8×10^{9} s^{-1} (for butanol) can be deduced from the transient absorption signals. The final constant of $k_{rel}^{S_0}$ refers to the ThT intramolecular structural and solvent relaxations necessary to reach the initial geometrical conformation of ThT in its relaxed ground state.

3.2. The Nonradiative Rate Constant of ThT. As mentioned above, Stsiapura et al.[38] and Amdursky et al.[32] have shown that the nonradiative rate constant of ThT, taking place in the excited state, $k_{LE\text{-}TICT}$, is highly dependent on the solvent viscosity. The second nonradiative process between S_1 and S_0, $k_{TICT\text{-}S_0}$, depends also on the solvent viscosity but is about 10 times slower. Table 2 shows the change in the nonradiative rate constant of ThT in several protic solvents with different viscosities. The measured nonradiative constant has been obtained through two different experimental setups: (1) Repopulation of the ground state, that is, the rate constant from the excited TICT state to the ground state was derived from transient absorption methods.[38] (2) The transition from the emissive LE to the dark TICT state was measured by time-resolved emission techniques.[31,32] The exceptionally strong dependence on the solvent viscosity of the nonradiative decay rate constant of ThT to the ground state can clearly be seen in Table 2. For example, a 2.5-fold increase in the solvent viscosity, from ethanol ($\eta_{ethanol} = 1.1$ cP) to butanol ($\eta_{butanol} = 2.7$ cP), results in a $\sim$13-fold decrease in the nonradiative rate constant, from 3.6×10^{10} to 2.8×10^{9} s^{-1} in the respective solvents.[38]

The change in the nonradiative rate as a function of the hydrostatic pressure[32] and temperature[31] were also reported. These observations directly confirm the viscosity dependence of the nonradiative rate, without the necessity of considering other, secondary, factors that might affect this

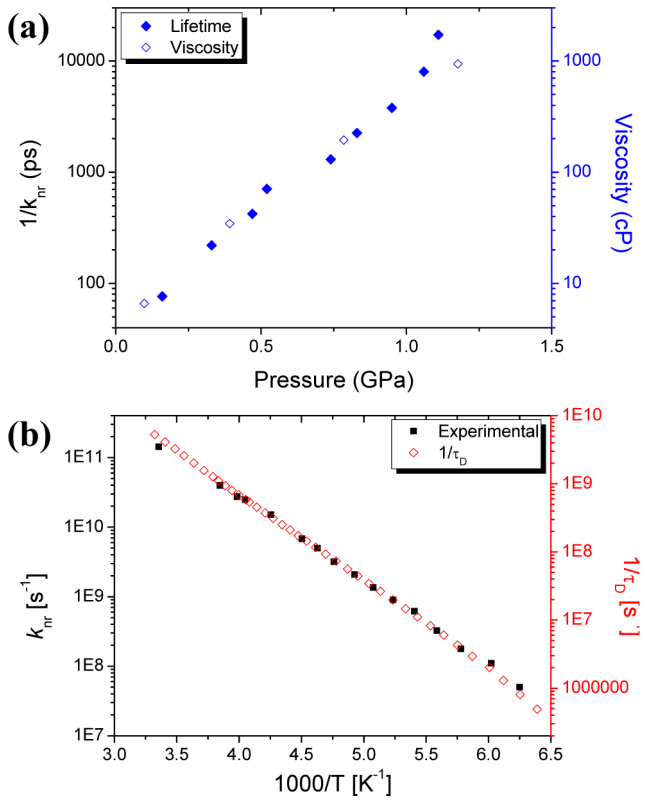

FIGURE 4. The change in the nonradiative rate constant as a function of (a) viscosity (in pentanol) and (b) temperature (in propanol). Reprinted with permission from refs 31 and 32. Copyright 2011 American Chemical Society.

rate that was obtained by the use of binary mixtures of viscous and nonviscous solvents.[30] The hydrostatic pressure influences the solution viscosity in a nonlinear way,[39] increasing it by a factor of 200−1000 at pressures of 1.2 GPa, for different protic solvents. Figure 4a shows the inverse of the nonradiative rate constant of ThT (equal to the nonradiative lifetime, $\tau_{nr} = 1/k_{nr}$, where k_{nr} is the nonradiative rate constant) and the solution viscosity as a function of the solution hydrostatic pressure. Large deviation from exponential decay prevents the use of a simple definition for the nonradiative rate constant; in such a barrierless transition, state mixing exists throughout the process to a varying extent. This is in contrast to a nonadiabatic process where a barrier exists, free crossing between states is prevented, and a rate constant can be defined.

It can be seen that the inverse of k_{nr} follows the changes in the viscosity at all pressures reasonably well. The changes in viscosity of approximately 2.5 orders of magnitude cause a remarkable change in the value of $1/k_{nr}$.

A more pronounced change in the nonradiative rate constant of ThT can be seen when the temperature of the solution (propanol) is changed.[31] The change in the viscosity of propanol with temperature follows its dielectric relaxation.[40] The dielectric relaxation measurements of Stickel et al.[40,41] show an increase of 11 orders of magnitude in the dielectric relaxation and viscosity of propanol when the temperature is lowered from room temperature to ∼100 K.

Figure 4b shows the values of k_{nr} of ThT in propanol, as calculated from the experimental results of the temperature study,[31] superimposed on the values of Stickel et al.[40,41] for propanol as a function of $1/T$ (over the range of 160−297 K). A remarkable fit of the nonradiative rate constant to the inverse of the dielectric relaxation time can be observed, over 3 orders of magnitude, from $k_{nr} = 5 \times 10^7$ s^{-1} (at $T = 160$ K) to 1.5×10^{11} s^{-1} (at $T = 297$ K). This fit is yet another indication of the molecular-rotor character of ThT, because it draws a clear dependence of the nonradiative decay rate on the viscosity of the solvent.

3.3. ThT as a Molecular Rotor. Schematically, one can visualize the rotation of the phenyl ring of ThT as the cause for the nonradiative processes.[31] The rotation of this phenyl ring from the dihedral angle of $\varphi = 37°$ (relative to the benzothiazole moiety) to $\varphi = 90°$ allows the transition in the excited state from the radiative LE state to the nonradiative TICT state. The rotation of an object rotating in viscous media has a rotational-relaxation time, τ_{rot}, given by

$$\tau_{rot} \cong \frac{\Delta\theta}{\Omega} \tag{1}$$

where Ω is the angular rotation velocity of the phenyl ring. The change in the twist angle of the phenyl ring between the two states, $\Delta\theta$, is about 1 rad, and thus $\tau_{rot} = 1/\Omega$. The angular rotation velocity, Ω, of the phenyl ring can be written as the torque multiplied by the angular mobility, μ:

$$\Omega = \mu \times \text{torque} \tag{2}$$

The torque is defined as

$$\text{torque} = \frac{\partial E}{\partial \theta} \tag{3}$$

where $\partial E/\partial\theta$ is the derivative of the potential energy with respect to the rotation angle of the phenyl ring. This value can be calculated from the potential-energy curve of the first excited state of ThT for the transition of $\varphi = 37°$ to 90° (Figure 3) and has a value of ∼200 meV (∼1600 cm^{-1}). The angular mobility, μ, can be expressed by the Einstein relation in a way similar to that for the

translational mobility of charged particles:

$$\mu = \frac{D_r}{kT} \tag{4}$$

where D_r is the rotational−diffusion coefficient. If we consider the rotational movement of the phenyl ring to be constrained to one rotational axis, the rotational diffusion can be express by:

$$2D_r = \frac{kT}{\eta V} \tag{5}$$

where η is the viscosity of the solvent and V is the volume of a rotating sphere. The integration of the above equations yields a final expression for τ_{rot}:

$$\tau_{rot} = \frac{1}{\mu \times \text{torque}} = \frac{2\eta V}{\text{torque}} \tag{6}$$

For a viscosity of 1 cP, a volume of the rotating phenyl group of ~20 Å^3, and a torque value of 200 meV/radian, a rotational-relaxation time of $\sim 10^{-12}$ s is obtained.

As described in section 2, the ThT fluorescence lifetime in water, for which $\eta = 1$ cP, is also about 1 ps. Thus, this simple, semiquantitative model of ThT as a molecular rotor fits well with the experimental emission lifetime of ThT. As pointed out in this Account, the nonradiative process of ThT depends on the solvent viscosity, as predicted by this model.

4. Existing Models for Nonradiative Processes

In order to model the nonradiative processes of ThT, we shall first review the existing nonradiative models that depend on an intramolecular coordinate. In this context, we will mention four main models: the Bagchi, Fleming, and Oxtoby (BFO) model,[42] the inhomogeneous model,[43] its Agmon−Hopfield diffusional extension,[44] and the Glasbeek model.[45]

4.1. The BFO Model. In 1986, Bagchi, Fleming, and Oxtoby[42] suggested a model for nonadiabatic curve crossing that involves nonradiative decay. The internal conversion (IC) of the nonadiabatic curve crossing occurs only at the intersection of the ground and excited potential curves. In this one-dimensional model, the initial population distribution, $p(x,0)$, diffuses toward the curve-crossing point and decays back to the ground state. The time delay between the initial excitation and the IC process is viscosity-dependent. Moreover, in highly viscous solvents, the distribution cannot diffuse to the intersection point, and no IC should occur. There is no reported observation that ThT fluorescence decay exhibits an initial delay and thus behaves according to the BFO model.

4.2. The Inhomogeneous Model. As mentioned above, the BFO model fails to predict the relatively fast subpicosecond to several tens of picoseconds multiexponential IC in viscous media, as shown experimentally.[46] The inhomogeneous model was successfully used by Agmon et al.[43] for *p*-hydroxybenzylidene dimethylimidazolinone (*p*-HBDI), a model compound for the green fluorescent protein chromophore. They used a nonlocal sink term, $k(z)$, that permits a nonradiative process not only at the curve-crossing point but for all molecular configurations. The model does not include diffusion and is intended for molecular systems in a frozen matrix. The *z*-coordinate is the twist angle between the two rings of *p*-HBDI. When the two rings are at 90°, the nonradiative rate is maximal. The nonradiative process is inhomogeneous since it occurs at all angles but at different rates, and therefore, instead of having a single rate constant, k_{nr}, there is a distribution of rates along the *z*-coordinate. A notable outcome is that the time-resolved emission modeled is nonexponential, since k_{nr} depends on the twist angle and the distribution of angles is relatively large. The inhomogeneous model cannot explain the large wavelength dependence of the decay rate of the time-resolved emission of ThT.

4.3. The Extended Inhomogeneous Model. The extension of the inhomogeneous model[44] incorporates into the original model a population-diffusion process along the excited-state potential curve toward the curve-crossing point. The nonradiative process influenced by diffusion can be described by the Agmon−Hopfield equation:[47]

$$\frac{\partial p(x,t)}{\partial t} = D\frac{\partial^2 p}{\partial x^2} + \frac{D}{k_B T}\frac{\partial}{\partial x}\left(p\frac{\partial V}{\partial x}\right) - k(x)p \tag{7}$$

where $p(x,t)$ represents the probability density of finding a value of p at time t, at a given value of x. The decay of $p(x,t)$ is affected by random diffusion, propagation under external potential, and an orthogonal process that consumes the excited population. Each of these processes is represented by one of the three terms on the right-hand side of the equation. When considering application of the extended inhomogeneous model for ThT, one should be cautious and note that for a diffusion constant that is not large, the population at time zero after impulse excitation is far from the crossing point coordinate, which is also the case for the BFO model. The inhomogeneous model also tends to increase the IC rate as time progresses, since it takes time for

the population to reach a closer "distance" to the crossing point, at which the IC rate is maximal. After excitation, the mean of the population-distribution function, $p(x,t)$, moves toward the crossing point, to the TICT state in the case of ThT.

4.4. The Glasbeek Model. The model that concludes this section is one that was first introduced by Glasbeek and co-workers for the nonradiative processes of auramine O.[45,48] Auramine O, like ThT, has a viscosity-dependent fluorescence quantum yield. This photophysical characteristic that must be taken into account in order to model the nonradiative processes of either auramine O or ThT makes the Glasbeek model an *a priori* promising candidate for ThT as well. In this model, the first molecular electronically excited singlet state is expressed as a mixture of two separate states, an emissive (F) state and a dark (D) state. Following a short excitation pulse, the initial population distribution resides in the F state and then diffuses by torsional motion toward the D state. The two diabatic states, F and D, are adiabatically coupled as a function of the normalized twist coordinate z:

$$S_1(z) = \frac{1}{2}[F(z) + D(z)] - \frac{1}{2}\sqrt{[F(z) - D(z)]^2 + 4C^2} \quad (8)$$

where C is the coupling-strength parameter. Such adiabatic coupling was introduced and used earlier by Fonseca, Barbara, and co-workers to model adiabatic excited-state electron-transfer processes, which depend on the solvent-reorganization coordinate, z. Since the S_1 state (of both auramine O and ThT) is a z-dependent mixture of radiative and nonradiative zero-order states, the transition dipole moment, $M(z)$, of the optical transition $S_1 \rightarrow S_0$ is also z-dependent. According to Glasbeek's model, the normalized $S_1 \rightarrow S_0$ transition dipole moment decreases as a function of z:

$$M(z) = \cos^2\left[\frac{1}{2}\arctan\left(\frac{2C}{F(z) - D(z)}\right)\right] \quad (9)$$

and the time-dependent fluorescence $I_{fl}(\nu,t)$, at time t and frequency ν exhibits the following proportionality:

$$I_{fl}(\nu,t) \propto \int dz\{g(\nu_0(z), \nu - \nu_0(z))|M(z)|^2 p(z,t)\nu^3\} \quad (10)$$

where $g(\nu_0(z), \nu - \nu_0(z))$ is a line-shape function characteristic of the Franck–Condon factor and $\nu_0(z)$ is the twist-angle-dependent energy gap between the excited and ground states. The population $p(z,t)$ was obtained by solving the Debye–Smoluchowski equation (an equation similar to eq 7, but without the third term on the right-hand side).

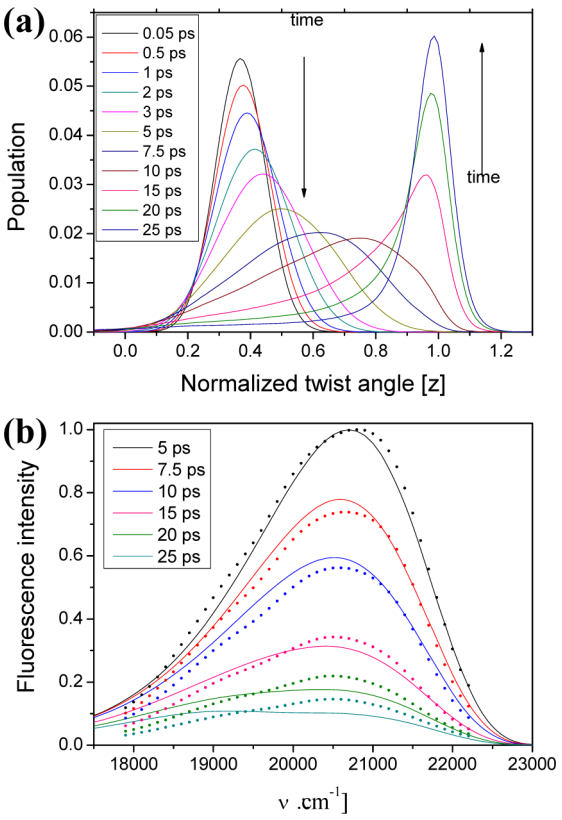

FIGURE 5. Modeling ThT according to Glasbeek model: (a) Calculated population distribution of ThT at several times as a function of the normalized twist angle. (b) Time-resolved emission spectra of ThT (dotted lines) at several times and its computed fits (solid lines). Reprinted with permission from ref 37. Copyright 2011 American Chemical Society.

The Glasbeek model was also used by Meech and co-workers[51] to quantify the torsional dynamics of auramine O. The change in the transition dipole moment of ThT as a function of the twist angle z was studied by quantum-molecular calculations, while taking into account the solvent effect by a conductor-like screening model,[28,30,35–37] where it was shown that the $S_1 \rightarrow S_0$ transition dipole moment decreases by a factor of ~100 as a function of the C–C dihedral angle (Figure 3b). When the Glasbeek model is applied to ThT, the minima of the $F(z)$ and $D(z)$ states should be assigned according to the ThT deactivation scheme with 90° (or $z = 1$) serving as the TICT nonemissive (D) state minimum and 37° serving as the ground-state minimum.

5. Modeling the Nonradiative Process of ThT on the Basis of the Glasbeek Model

For the modeling of the nonradiative process of ThT, the Debye–Smoluchowski equation was used to compute

the time-dependent population-distribution function, $p(z,t)$ (Figure 5a) along the excited-state-potential curve of ThT (Figure 3a).[37] The calculation showed that the population is redistributed with time and shifts from an initial peak position at $z = 0.37$ toward the minimum of the potential curve at $z = 1$, where the twist angle between the two ring systems is 90°. The time-dependent experimental fluorescence-band energy shift of ThT in propanol from $\tau \approx 0.5$ to 20 ps is ~2100 cm^{-1}, whereas the calculated maximum band shift is ~3700 cm^{-1} (Figure 5a).

The twisting of the aniline with respect to the benzothiazole ring not only reduces the fluorescence energy but also mixes the LE state with the CT state, thus reducing the transition dipole moment, $M(z)$, and the oscillator strength, f (Figure 3b). Since the CT state is a "dark" state, the transfer of the population leads to fluorescence decay at a rate that depends on both the rotational-diffusion constant, D_r, and the slope of the potential curve (the torque in eqs 3 and 6).

The experimental time-resolved emission spectra of ThT have also been modeled (Figure 5b) with several parameters that had to be considered:[37] (1) The log-normal parameters for the Franck−Condon spectral line shape of the spectrum. (2) The total red shift of the spectra as a function of z. This parameter is calculated from the energy of the gap between the $S_1(z)$ and $S_0(z)$ states of the spectra as a function of z. (3) D_r of the ring system, which is dependent on the macroscopic shear-diffusion constant of the solvent. (4) The decay time of the TICT state to the ground state of ThT in propanol.

While the time-dependence of the intensity decrease of the emission spectra at intermediate and long times ($t \geq 5$ ps) is well accounted by the model, the experimental results at short times ($t < 5$ ps) could only be fit with the use of a 3.3 times larger value of D_r. The rotational-diffusion coefficient, $D_r = 0.1$ ps^{-1}, obtained for the best fit for the long times, is consistent with the value predicted by calculation of a phenyl size rotating object in a viscous medium with $\eta = 2.4$ cP, the value for propanol. The faster-decaying components observed for the short times could be explained by solvation dynamics taking place prior to and during aniline rotation. As a consequence, a time-dependent Stokes shift takes place.

Meech and co-workers[51−53] found that the time-resolved fluorescence spectrum of auramine O, like that of ThT, also consists of two time components. The band-shift rate of the first moment of the fluorescence as well as the rate of loss of fluorescence intensity is faster at short times. Accurate fitting of the time-resolved emission spectra of auramine O was achieved with the use of a time-dependent diffusion coefficient, $D(t)$, rather than one independent of time. They suggested that the diffusion time dependence arises from the medium's time-dependent friction, reflecting dynamics over a broad range of time scales. The formal definition of $D(t)$ for a certain potential-energy surface was given earlier in the works of Hynes and co-workers[54,55] and of Oxtoby and co-workers.[56,57]

6. Conclusions

In this Account, we have discussed the unique photophysical properties of ThT, which is mainly used as a fluorescent marker for amyloid fibrils. The increased emission intensity of ThT upon binding to amyloid fibrils is due to the inhibition of the rotation around a single C−C bond in ThT, which causes the electronic wave function in the excited state to change adiabatically from an emissive LE state to a dark (nonradiative) CT state. This rotation-dependent TICT behavior is what defines ThT as a fluorescent molecular rotor. The rotation around this bond may be hindered not only by adsorption to amyloid fibrils but also by increase in solvent viscosity. By controlling the viscosity of the molecule's microenvironment, the nonradiative decay can be reduced by many orders of magnitude. Further, we discuss the nonradiative process of ThT in the context of several known nonradiative models. Among these, we focused on a model proposed by Glasbeek and show how the nonradiative decay of ThT can be modeled and fitted according to it. In this light, we believe that this Account provides insight on the broader context subject of characteristic behavior of molecular rotors.

BIOGRAPHICAL INFORMATION

Nadav Amdursky received a B.Sc. in Biotechnology from Tel Aviv University and continued there for his graduate studies at the departments of Physical Electronics and Biotechnology, where he focused on the optical and dielectric properties of peptide structures. He is currently working as a postdoctoral fellow at the Weizmann Institute of Science, where he focuses on solid state electron transport across proteins.

Yuval Erez received a B.Sc. in Chemistry and Computer Science and a M.Sc. in Chemistry from the Tel Aviv University. In his Master's studies, he focused on the isolation and structure elucidation of natural products from marine origin. He is currently a Ph.D. student at the Tel Aviv University where he studies competing processes in the excited state.

Dan Huppert received a B.Sc. and a Ph.D. (1974) in Chemistry from the Tel Aviv University and was a postdoctoral fellow at Bell Laboratories. Since 1977, he has been a faculty member of the Tel Aviv University, where he employs ultrafast spectroscopy to study excited-state proton transfer reactions in solutions and in GFP proteins.

FOOTNOTES

The authors declare no competing financial interest.

REFERENCES

1 Rogers, D. R. Screening for Amyloid with Thioflavin-T Fluorescent Method. *Am. J. Clin. Pathol.* **1965**, *44*, 59.

2 Sulatskaya, A. I.; Kuznetsova, I. M.; Turoverov, K. K. Interaction of Thioflavin T with Amyloid Fibrils: Stoichiometry and Affinity of Dye Binding, Absorption Spectra of Bound Dye. *J. Phys. Chem. B* **2011**, *115*, 11519–11524.

3 Sulatskaya, A. I.; Kuznetsova, I. M.; Turoverov, K. K. Interaction of Thioflavin T with Amyloid Fibrils: Fluorescence Quantum Yield of Bound Dye. *J. Phys. Chem. B* **2012**, *116*, 2538–2544.

4 Naiki, H.; Higuchi, K.; Hosokawa, M.; Takeda, T. Fluorometric-Determination of Amyloid Fibrils Invitro Using the Fluorescent Dye, Thioflavine-T. *Anal. Biochem.* **1989**, *177*, 244–249.

5 Klunk, W. E.; Wang, Y. M.; Huang, G. F.; Debnath, M. L.; Holt, D. P.; Mathis, C. A. Uncharged Thioflavin-T Derivatives Bind to Amyloid-beta Protein with High Affinity and Readily Enter the Brain. *Life Sci.* **2001**, *69*, 1471–1484.

6 Mathis, C. A.; Bacskai, B. J.; Kajdasz, S. T.; McLellan, M. E.; Frosch, M. P.; Hyman, B. T.; Holt, D. P.; Wang, Y. M.; Huang, G. F.; Debnath, M. L.; Klunk, W. E. A Lipophilic Thioflavin-T Derivative for Positron Emission Tomography (PET) Imaging of Amyloid in Brain. *Bioorg. Med. Chem. Lett.* **2002**, *12*, 295–298.

7 LeVine, H. Quantification of beta-Sheet Amyloid Fibril Structures with Thioflavin T. *Methods Enzymol.* **1999**, *309*, 274–284.

8 Ban, T.; Hamada, D.; Hasegawa, K.; Naiki, H.; Goto, Y. Direct Observation of Amyloid Fibril Growth Monitored by Thioflavin T Fluorescence. *J. Biol. Chem.* **2003**, *278*, 16462–16465.

9 Bulic, B.; Pickhardt, M.; Schmidt, B.; Mandelkow, E. M.; Waldmann, H.; Mandelkow, E. Development of Tau Aggregation Inhibitors for Alzheimer's Disease. *Angew. Chem., Int. Ed.* **2009**, *48*, 1741–1752.

10 Cundall, R. B.; Davies, A. K.; Morris, P. G.; Williams, J. Factors Influencing the Photosensitizing Properties and Photo-Luminescence of Thioflavin-T. *J. Photochem.* **1981**, *17*, 369–376.

11 Ilanchelian, M.; Ramaraj, R. Emission of Thioflavin T and Its Control in the Presence of DNA. *J. Photochem. Photobiol., A* **2004**, *162*, 129–137.

12 Raj, C. R.; Ramaraj, R. Influence of Cyclodextrin Complexation on the Emission of Thioflavin T and Its off-on Control. *J. Photochem. Photobiol., A* **1999**, *122*, 39–46.

13 Choudhury, S. D.; Mohanty, J.; Upadhyaya, H. P.; Bhasikuttan, A. C.; Pal, H. Photophysical Studies on the Noncovalent Interaction of Thioflavin T with Cucurbit[n]uril Macrocycles. *J. Phys. Chem. B* **2009**, *113*, 1891–1898.

14 Raj, C. R.; Ramaraj, R. Emission of Thioflavin T and its off-on control in polymer Membranes. *Photochem. Photobiol.* **2001**, *74*, 752–759.

15 Kumar, S.; Singh, A. K.; Krishnamoorthy, G.; Swaminathan, R. Thioflavin T Displays Enhanced Fluorescence Selectively Inside Anionic Micelles and Mammalian Cells. *J. Fluoresc.* **2008**, *18*, 1199–1205.

16 Hutter, T.; Amdursky, N.; Gepshtein, R.; Elliott, S. R.; Huppert, D. Study of Thioflavin-T Immobilized in Porous Silicon and the Effect of Different Organic Vapours on the Fluorescence Lifetime. *Langmuir* **2011**, *27*, 7587–7594.

17 Biancalana, M.; Koide, S. Molecular Mechanism of Thioflavin-T Binding to Amyloid Fibrils. *Biochim. Biophys. Acta, Proteins Proteomics* **2010**, *1804*, 1405–1412.

18 Groenning, M. Binding mode of Thioflavin T and Other Molecular Probes in the Context of Amyloid Fibrils—Current Status. *J. Chem. Biol.* **2010**, *3*, 1–18.

19 Harel, M.; Sonoda, L. K.; Silman, I.; Sussman, J. L.; Rosenberry, T. L. Crystal Structure of Thioflavin T Bound to the Peripheral Site of *Torpedo californica* Acetylcholinesterase Reveals How Thioflavin T Acts as a Sensitive Fluorescent Reporter of Ligand Binding to the Acylation Site. *J. Am. Chem. Soc.* **2008**, *130*, 7856–7861.

20 Khurana, R.; Coleman, C.; Ionescu-Zanetti, C.; Carter, S. A.; Krishna, V.; Grover, R. K.; Roy, R.; Singh, S. Mechanism of Thioflavin T Binding to Amyloid Fibrils. *J. Struct. Biol.* **2005**, *151*, 229–238.

21 Krebs, M. R. H.; Bromley, E. H. C.; Donald, A. M. The Binding of Thioflavin-T to Amyloid Fibrils: Localisation and Implications. *J. Struct. Biol.* **2005**, *149*, 30–37.

22 Wu, C.; Biancalana, M.; Koide, S.; Shea, J. E. Binding Modes of Thioflavin-T to the Single-Layer beta-Sheet of the Peptide Self-Assembly Mimics. *J. Mol. Biol.* **2009**, *394*, 627–633.

23 Kitts, C. C.; Bout, D. A. V. Near-Field Scanning Optical Microscopy Measurements of Fluorescent Molecular Probes Binding to Insulin Amyloid Fibrils. *J. Phys. Chem. B* **2009**, *113*, 12090–12095.

24 Schirra, R. Dye Aggregation in Freezing Aqueous-Solutions. *Chem. Phys. Lett.* **1985**, *119*, 463–466.

25 Voropai, E. S.; Samtsov, M. P.; Kaplevskii, K. N.; Maskevich, A. A.; Stepuro, V. I.; Povarova, O. I.; Kuznetsova, I. M.; Turoverov, K. K.; Fink, A. L.; Uverskii, V. N. Spectral Properties of Thioflavin T and Its Complexes with Amyloid Fibrils. *J. Appl. Spectrosc.* **2003**, *70*, 868–874.

26 Maskevich, A. A.; Stsiapura, V. I.; Kuzmitsky, V. A.; Kuznetsova, I. M.; Povarova, O. I.; Uversky, V. N.; Turoverov, K. K. Spectral Properties of Thioflavin T in Solvents with Different Dielectric Properties and in a Fibril-Incorporated Form. *J. Proteome Res.* **2007**, *6*, 1392–1401.

27 Naik, L. R.; Naik, A. B.; Pal, H. Steady-State and Time-Resolved Emission Studies of Thioflavin-T. *J. Photochem. Photobiol., A* **2009**, *204*, 161–167.

28 Stsiapura, V. I.; Maskevich, A. A.; Kuzmitsky, V. A.; Uversky, V. N.; Kuznetsova, I. M.; Turoverov, K. K. Thioflavin T as a Molecular Rotor: Fluorescent Properties of Thioflavin T in Solvents with Different Viscosity. *J. Phys. Chem. B* **2008**, *112*, 15893–15902.

29 Sulatskaya, A. I.; Maskevich, A. A.; Kuznetsova, I. M.; Uversky, V. N.; Turoverov, K. K. Fluorescence Quantum Yield of Thioflavin T in Rigid Isotropic Solution and Incorporated into the Amyloid Fibrils. *PLoS One* **2010**, *5*, No. e15385.

30 Singh, P. K.; Kumbhakar, M.; Pal, H.; Nath, S. Viscosity Effect on the Ultrafast Bond Twisting Dynamics in an Amyloid Fibril Sensor: Thioflavin-T. *J. Phys. Chem. B* **2010**, *114*, 5920–5927.

31 Amdursky, N.; Gepshtein, R.; Erez, Y.; Huppert, D. Temperature Dependence of the Fluorescence Properties of Thioflavin-T in Propanol, a Glass-Forming Liquid. *J. Phys. Chem. A* **2011**, *115*, 2540–2548.

32 Amdursky, N.; Gepshtein, R.; Erez, Y.; Koifman, N.; Huppert, D. Pressure Effect on the Nonradiative Process of Thioflavin-T. *J. Phys. Chem. A* **2011**, *115*, 6481–6487.

33 Singh, P. K.; Kumbhakar, M.; Pal, H.; Nath, S. Ultrafast Torsional Dynamics of Protein Binding Dye Thioflavin-T in Nanoconfined Water Pool. *J. Phys. Chem. B* **2009**, *113*, 8532–8538.

34 Kuznetsova, I. M.; Sulatskaya, A. I.; Uversky, V. N.; Turoverov, K. K. Analyzing Thioflavin T Binding to Amyloid Fibrils by an Equilibrium Microdialysis-Based Technique. *PLoS One* **2012**, *7*, No. e30724.

35 Singh, P. K.; Kumbhakar, M.; Pal, H.; Nath, S. Ultrafast Bond Twisting Dynamics in Amyloid Fibril Sensor. *J. Phys. Chem. B* **2010**, *114*, 2541–2546.

36 Stsiapura, V. I.; Maskevich, A. A.; Kuzmitsky, V. A.; Turoverov, K. K.; Kuznetsova, I. M. Computational Study of Thioflavin T Torsional Relaxation in the Excited State. *J. Phys. Chem. A* **2007**, *111*, 4829–4835.

37 Erez, Y.; Liu, Y. H.; Amdursky, N.; Huppert, D. Modeling the Nonradiative-Decay Rate of Electronically-Excited ThT. *J. Phys. Chem. A* **2011**, *115*, 8479–8487.

38 Stsiapura, V. I.; Maskevich, A. A.; Tikhomirov, S. A.; Buganov, O. V. Charge Transfer Process Determines Ultrafast Excited State Deactivation of Thioflavin T in Low-Viscosity Solvents. *J. Phys. Chem. A* **2010**, *114*, 8345–8350.

39 Bridgman, P. W. *The Physics of High Pressure*; Dover Publications, Inc.: New York, 1970.

40 Hansen, C.; Stickel, F.; Berger, T.; Richert, R.; Fischer, E. W. Dynamics of Glass-Forming Liquids. 3. Comparing the Dielectric alpha- and beta-Relaxation of 1-Propanol and o-Terphenyl. *J. Chem. Phys.* **1997**, *107*, 1086–1093.

41 Richert, R.; Stickel, F.; Fee, R. S.; Maroncelli, M. Solvation Dynamics and the Dielectric Response in a Glass-Forming Solvent - from Picoseconds to Seconds. *Chem. Phys. Lett.* **1994**, *229*, 302–308.

42 Bagchi, B.; Fleming, G. R.; Oxtoby, D. W. Theory of Electronic Relaxation in Solution in the Absence of an Activation Barrier. *J. Chem. Phys.* **1983**, *78*, 7375–7385.

43 Gepshtein, R.; Huppert, D.; Agmon, N. Deactivation Mechanism of the Green Fluorescent Chromophore. *J. Phys. Chem. B* **2006**, *110*, 4434–4442.

44 Radoszkowicz, L.; Presiado, I.; Erez, Y.; Nachliel, E.; Huppert, D.; Gutman, M. Time-Resolved Emission of Flavin Adenine Dinucleotide in Water and Water-Methanol Mixtures. *Phys. Chem. Chem. Phys.* **2011**, *13*, 12058–12066.

45 van der Meer, M. J.; Zhang, H.; Glasbeek, M. Femtosecond Fluorescence Upconversion Studies of Barrierless Bond Twisting of Auramine in Solution. *J. Chem. Phys.* **2000**, *112*, 2878–2887.

46 Kummer, A. D.; Kompa, C.; Niwa, H.; Hirano, T.; Kojima, S.; Michel-Beyerle, M. E. Viscosity-Dependent Fluorescence Decay of the GFP Chromophore in Solution Due to Fast Internal Conversion. *J. Phys. Chem. B* **2002**, *106*, 7554–7559.

47 Agmon, N.; Hopfield, J. J. Transient Kinetics of Chemical-Reactions with Bounded Diffusion Perpendicular to the Reaction Coordinate - Intramolecular Processes with Slow Conformational-Changes. *J. Chem. Phys.* **1983**, *78*, 6947–6959.

48 Glasbeek, M.; Zhang, H. Femtosecond Studies of Solvation and Intramolecular Configurational Dynamics of Fluorophores in Liquid Solution. *Chem. Rev.* **2004**, *104*, 1929–1954.

49 Tominaga, K.; Walker, G. C.; Jarzeba, W.; Barbara, P. F. Ultrafast charge Separation in ADMA: Experiment, Simulation, And Theoretical Issues. *J. Phys. Chem.* **1991**, *95*, 10475–10485.

50 Tominaga, K.; Walker, G. C.; Kang, T. J.; Barbara, P. F.; Fonseca, T. Reaction Rates in the Phenomenological Adiabatic Excited-State Electron-Transfer Theory. *J. Phys. Chem.* **1991**, *95*, 10485–10492.

51 Heisler, I. A.; Kondo, M.; Meech, S. R. Reactive Dynamics in Confined Liquids: Ultrafast Torsional Dynamics of Auramine O in Nanoconfined Water in Aerosol OT Reverse Micelles. *J. Phys. Chem. B* **2009**, *113*, 1623–1631.

52 Kondo, M.; Heisler, I. A.; Conyard, J.; Rivett, J. P. H.; Meech, S. R. Reactive Dynamics in Confined Liquids: Interfacial Charge Effects on Ultrafast Torsional Dynamics in Water Nanodroplets. *J. Phys. Chem. B* **2009**, *113*, 1632–1639.

53 Kondo, M.; Heisler, I. A.; Meech, S. R. Reactive Dynamics in Micelles: Auramine O in Solution and Adsorbed on Regular Micelles. *J. Phys. Chem. B* **2010**, *114*, 12859–12865.

54 Vanderzwan, G.; Hynes, J. T. Dynamical Polar Solvent Effects on Solution Reactions: A Simple Continuum Model. *J. Chem. Phys.* **1982**, *76*, 2993–3001.

55 Vanderzwan, G.; Hynes, J. T. Nonequilibrium Solvation Dynamics in Solution Reactions. *J. Chem. Phys.* **1983**, *78*, 4174–4185.

56 Okuyama, S.; Oxtoby, D. W. The Generalized Smoluchowski Equation and Non-Markovian Dynamics. *J. Chem. Phys.* **1986**, *84*, 5824–5829.

57 Okuyama, S.; Oxtoby, D. W. Non-Markovian Dynamics and Barrier Crossing Rates at High Viscosity. *J. Chem. Phys.* **1986**, *84*, 5830–5835.